NATIONAL ADVISORY COMMITTEE FOR AERONAUTICS

WARTIME REPORT

ORIGINALLY ISSUED

May 1944 as
Advance Restricted Report L4E27

THE EFFECT OF INTERNAL PRESSURE ON THE BUCKLING STRESS OF THIN-WALLED CIRCULAR CYLINDERS UNDER TORSION

By Harold Crate, S. B. Batdorf, and George W. Baab

Langley Memorial Aeronautical Laboratory
Langley Field, Va.

PROPERTY OF JET PROPULSION LABORATORY LIBRARY
CALIFORNIA INSTITUTE OF TECHNOLOGY

JPL LIBRARY
CALIFORNIA INSTITUTE OF TECHNOLOGY

NACA

WASHINGTON

NACA WARTIME REPORTS are reprints of papers originally issued to provide rapid distribution of advance research results to an authorized group requiring them for the war effort. They were previously held under a security status but are now unclassified. Some of these reports were not technically edited. All have been reproduced without change in order to expedite general distribution.

NATIONAL ADVISORY COMMITTEE FOR AERONAUTICS

ADVANCE RESTRICTED REPORT

THE EFFECT OF INTERNAL PRESSURE ON THE BUCKLING STRESS OF THIN-WALLED CIRCULAR CYLINDERS UNDER TORSION

By Harold Crate, S. B. Batdorf, and George W. Baab

SUMMARY

The results of a series of tests to determine the effect of internal pressure on the buckling load of a thin cylinder under an applied torque indicated that internal pressure raises the shear buckling stress. The experimental results were analyzed with the aid of previously developed theory and a simple interaction formula was derived.

INTRODUCTION

The curved metal skin of a modern airplane in flight is subject to stresses that may cause the skin to buckle, and proper design of airplane structures requires a knowledge of the stress conditions under which buckling will occur. The ability to estimate the buckling point under combined loading conditions is of particular importance.

In order to determine the effect that normal pressure, or air loads, might have on the critical stress for curved sheet, two preliminary tests were made (refences 1 and 2). A pronounced increase in critical stress with increase in normal pressure was found, and the subsequent interest shown by the aircraft industry in this subject indicated the desirability of further study.

No well-established theories for buckling of curved-sheet panels either in torsion or under hydrostatic pressure are available; however, satisfactory theories for buckling of complete cylinders under these loadings have been advanced (references 3 and 4). In order to effect some correlation between theory and experiment,

JPL LIBRARY
CALIFORNIA INSTITUTE OF TECHNOLOGY

therefore, an investigation was made of the influence of internal pressure on the critical stresses of thin cylinders in torsion. Experiments were conducted to determine the critical shear stresses for four cylinder lengths at a number of different internal pressures. The theories and the experimental data were used in conjunction to determine an interaction formula for the buckling of cylinders of moderate length under the combined action of torsion and internal pressure.

SYMBOLS

E	Young's modulus of elasticity, psi
G	shear modulus of elasticity, psi
L_o	length of cylinder without rings, inches
L	length of cylinder between rings, inches
t	thickness of cylinder wall, inches
d	diameter of cylinder, inches
r	radius of cylinder, inches
p	internal pressure of cylinder, considered positive when it produces tensile stresses in cylinder walls, psi
$(p_{cr})_{\tau=0}$	critical pressure in the absence of torsion (negative according to sign convention adopted for p), psi
τ	shear stress in cylinder walls due to applied torque, psi
τ_{cr}	value of shear stress when cylinder is at the point of elastic instability, psi
$(\tau_{cr})_{p=0}$	critical shear stress in the absence of internal pressure, psi
R_p	pressure ratio $\left(\frac{p}{(p_{cr})_{\tau=0}}\right)$

R_s shear-stress ratio $\left(\frac{\tau_{cr}}{(\tau_{cr})_{p=0}}\right)$

q exponent of R_s in the interaction formula

θ rotation of free end of cylinder, radians

K_s coefficient used in Lundquist's empirical formula (appendix A)

y, y_1 differences in strain gage readings

μ Poisson's ratio

SPECIMENS AND TEST PROCEDURE

Diagrams of the test-cylinder construction and ring systems used are given in figure 1. The cylinder was made from 0.032-inch 24S-T aluminum-alloy sheet closely riveted around two heavy steel rings, one at each end. The sheet was joined along an element of the cylinder with a butt joint covered with a single strap on the outside. Rings made of 24S-T aluminum alloy were added to this cylinder and divided it into shorter cylinders, the lengths of which were equal to the ring spacings.

Figure 2 is a photograph of the apparatus used to test the cylinder. The ends of the cylinder were closed by heavy flat steel plates in order that air could be maintained under pressure inside the cylinder. The weights of the steel plate and test ring at the free end of the cylinder were neutralized by an upward load on one of the torque arms. Rotations of the free end of the cylinder relative to the floor were measured by a pair of dial gages.

Observed buckling loads at zero and at low internal pressure were determined as the loads at which there was a sudden snap of the cylinder to the buckled state. This snap action was in many cases preceded by a slow growth of visible wrinkles in the cylinder walls as the load increased and a greatly increased rate of growth of the wrinkles at close proximity to the snap-buckling load. With increases in the internal pressure, the

snap decreased in violence until it was no longer observable. In these cases the buckling load was estimated, on the basis of visual observations, to be that load at which the rate of growth of wrinkles with load was comparable with the rate of growth of wrinkles just prior to buckling in those cases in which snap buckling did occur.

The Southwell method of determining the critical stress of specimens with initial eccentricities was assumed to be applicable to cylinders subjected to torsion and was used as a check on the visual determination. Two electrical strain gages were mounted on opposite sides of the cylinder wall at the crest of a buckle, the location of which was determined by means of a preliminary buckling test. The difference y in readings of the strain gages on opposite sides of the cylinder wall provided a numerical measure of the distortion as the wrinkles grew. The Southwell method was applied by plotting $(y - y_1)/(\tau - \tau_1)$ against $y - y_1$ where y_1 and τ_1 were arbitrarily chosen initial values of each quantity (reference 5). The inverse slope of the straight line formed in this manner is $\tau_{cr} - \tau_1$ where τ_{cr} is the desired critical stress.

DISCUSSION OF RESULTS

In figure 3 the shear stress calculated from the external load on the cylinder is plotted against the corresponding rotation of the free end for various values of ring spacing and internal pressure. The solid lines give rotations computed by the formula

$$\theta = \frac{\tau}{G} \frac{2L_o}{d}$$

in which G was assumed to be 3,970,000 psi.

Prior to buckling, the stiffness of the cylinder in torsion (slope of the curves) is essentially unaffected by the internal pressure or by the ring spacing. The rotations measured were slightly greater than those predicted by the formula. This result may be attributed

to the method of measurement, which considered as rotations many other small effects, such as bending of the column supporting the cylinder, distortion of rivets and rivet holes, and taking up slack in the bolt holes in the end plates.

The experimental buckling stress in torsion without pressure is compared with the predictions of Donnell (reference 3) and Lundquist (reference 6) in the following table:

L/d	Critical shear stress, ksi		
	Experimental	Lundquist	Donnell
0.18	5.8	6.0	7.9
.36	3.9	4.2	4.9
.72	3.0	3.0	3.3
1.43	2.3	2.3	2.3

Lundquist's formula was derived for stress at failure. Except for very short cylinders, however, the shear buckling stress and the stress at failure are essentially the same. Donnell's theoretical curve (solid curve of fig. 4) and Lundquist's empirical formula are discussed more fully in appendix A.

In figure 5 the buckling stresses under torsion are plotted against the internal pressure for each cylinder; this figure indicates that the buckling stresses increase as pressure increases. The results were essentially the same whether the visual or the Southwell method of determining buckling loads was used, although the Southwell method usually gave slightly higher loads than the visual.

The buckled cylinder could be returned to the unbuckled state either by decreasing the torque or by increasing the pressure. The loads at which the buckles disappeared were determined visually for cylinders 1, 2, and 3a, and are also shown in figure 5. These loads were not recorded, however, for the remaining cylinders because of a large scatter in the readings. This

scatter is attributable to the fact that, as the cylinders became shorter, the disappearance of the buckles became more gradual and the visual selection of a "point of disappearance" became difficult. In the case of cylinder 2, in which the readings are relatively definite, the location of the curve indicating disappearance of buckles was the same for either an increase of pressure or a reduction of torsion.

The method used to find the interaction formula best representing the experimental data is given in appendix A. The analysis leads to a formula of the type

$$R_s^{\,q} + R_p = 1$$

where the value of the exponent q depends upon the assumptions made for $(p_{cr})_{\tau=0}$ and $(\tau_{cr})_{p=0}$. For cylinders of moderate length, which according to Donnell's analysis satisfy the inequality

$$30\frac{t}{d} < \left(\frac{L}{d}\right)^2 < 5\frac{d}{t}$$

the exponent q is equal to 1.89 to 2 using τ_{cr} derived from Donnell's theoretical curve, the exact value depending on the value of L^2/td concerned. When τ_{cr} derived from Lundquist's empirical formula is used, $q = 2.17$.

In figure 6, curves representing the exponents 1.89, 2, and 2.17 are drawn through the experimental data of figure 5 replotted by a method explained in appendix A. The three curves lie close together and, so far as fit of data is concerned, little basis exists for a choice among them. Simplicity and proximity to the average value, however, recommend use of $q = 2$. The equation then becomes

$$R_s^{\,2} + R_p = 1$$

The parameter L^2/td, which according to theory determines buckling behavior, may be varied by changing the length, thickness, diameter, or any combination of dimensions. For this reason, the restriction of the tests to one thickness and one diameter probably does not constitute a significant loss in generality.

The question of the applicability of the formula to curved panels is discussed briefly in appendix B.

CONCLUSION

The critical stress of a cylinder in torsion increases as the internal pressure increases. The following interaction formula was found to represent approximately the buckling of a cylinder of moderate length under the combined effects of torsion and internal pressure:

$$R_s^2 + R_p = 1$$

where R_s is the ratio of critical shear stress with internal pressure to critical shear stress without internal pressure and R_p is the ratio of internal pressure to the critical pressure in the absence of torsion.

Langley Memorial Aeronautical Laboratory,
National Advisory Committee for Aeronautics,
Langley Field, Va.

APPENDIX A

DERIVATION OF INTERACTION FORMULA

Introductory Discussion

Any attempt to determine which of the conventional types of interaction formulas best fits the experimental data presented in this paper is complicated by the question of which values to use for $(p_{cr})_{\tau=0}$ and $(\tau_{cr})_{p=0}$. Experimental values for $(\tau_{cr})_{p=0}$ were obtained, but the corresponding experimental values of $(p_{cr})_{\tau=0}$ were not investigated because of the destructive effects on the cylinder involved in such a test. A simple experimental result makes possible a derivation of an interaction formula without necessitating assumptions concerning stress ratios or the type of formula to be used.

The experimental data appear to indicate that the interaction curves for the four cylinders tested are identical, differing only in position. (See fig. 5.) The effect of a change of length appears to be a shift of the curve parallel to the pressure axis. In figure 6 this effect is made clearer by plotting all the data to a common p-intercept. The curve for $\frac{L}{d} = 1.43$ is shifted parallel to the p-axis a distance equal to $-(p_{cr})_{\tau=0}$ (as given by equation (5) which follows) in order to make the p-intercept zero. Each of the other curves is then shifted the proper distance for best superposition. The relatively slight scatter shows that the experimental curves are nearly superposable.

If it is assumed that the interaction curves for different lengths of cylinder are for practical purposes identical, a computation of the equation for the curves from theory is possible. Among the points on the curve of figure 6 are four, indicated by modified symbols, representing the special case $p = 0$ for the four values of the length. Because the curve of figure 7 represents τ_{cr} plotted against $p - (p_{cr})_{\tau=0}$, these four points represent $(\tau_{cr})_{p=0}$ plotted against $-(p_{cr})_{\tau=0}$

for various values of the length. The formula for this curve can therefore be obtained by eliminating the length from the equations expressing $(\tau_{cr})_{p=0}$ and $(p_{cr})_{\tau=0}$ in terms of L, d, and t. The interaction curve for a cylinder of given dimensions can then be obtained by shifting the origin to make the p-intercept equal to $(p_{cr})_{\tau=0}$ for that cylinder. The interaction formula may then be derived by finding simplified expressions for $(\tau_{cr})_{p=0}$ and $(p_{cr})_{\tau=0}$, eliminating L, and transforming to give the final formula.

Simplified Expressions for $(\tau_{cr})_{p=0}$

Two simplified expressions for $(\tau_{cr})_{p=0}$ are derived, the first based on Donnell's curve (reference 3) and the other on Lundquist's formula (reference 6).

Donnell's theoretical result for the shear buckling stress of thin-walled cylinders with simply supported ends subjected to torsion is given by the solid curve of figure 4. For cylinders of moderate length, the curve is nearly a straight line given by the equation

$$(\tau_{cr})_{p=0} = 1.4E\left(\frac{L}{d}\right)^{-0.53}\left(\frac{d}{t}\right)^{-1.265} \tag{1a}$$

while for extremely large values of L^2/td a better fit is given by the equation of the asymptote

$$(\tau_{cr})_{p=0} = 1.27E\left(\frac{L}{d}\right)^{-0.5}\left(\frac{d}{t}\right)^{-1.25} \tag{1b}$$

This essentially straight portion of the curve is included between the limits

$$30\frac{t}{d} < \left(\frac{L}{d}\right)^2 < 5\frac{d}{t} \tag{2}$$

At the lower limit of inequality (2), equation (1a) is in error by about 15 percent and equation (1b), by about 20 percent. (For the upper limit see reference 3.)

Lundquist's formula is

$$(\tau_{cr})_{p=0} = K_s E\left(\frac{r}{t}\right)^{-1.35}$$

where values of K_s are given in reference 6 for various values of L/r. In order to determine a formula for K_s, the values of K_s were plotted against L/r on logarithmic paper. (See fig. 7.) When $L/r > 0.5$,

$$K_s = 1.27\left(\frac{L}{r}\right)^{-0.46}$$

At $L/r = 0.35$ (approximately the lower limit of inequality (2) for the cylinder tested), the error in this formula is about 7 percent. Use of this value of K_s leads to the formula

$$\tau_{cr\ p=0} = 2.36E\left(\frac{L}{d}\right)^{-0.46}\left(\frac{d}{t}\right)^{-1.35} \tag{3}$$

Simplified Expression for $(p_{cr})_{\tau=0}$

A formula based on work by von Mises and developed at the David Taylor Model Basin (equation (10) of reference 7) for the buckling of a closed cylinder under hydrostatic pressure may be written

$$-(p_{cr})_{\tau=0} = \frac{2.60E\frac{d}{L}\left(\frac{t}{d}\right)^{2.5}}{1 - 0.45\frac{d}{L}\left(\frac{t}{d}\right)^{0.5}} \tag{4}$$

If, as in the inequality (2),

$$30\frac{t}{d} < \left(\frac{L}{d}\right)^2$$

the denominator of equation (4) remains within 10 percent of unity, so that, to this degree of approximation,

$$-(p_{cr})_{\tau=0} = 2.60E\frac{d}{L}\left(\frac{t}{d}\right)^{2.5} \tag{5}$$

The negative sign appears because in the present paper internal pressure is considered positive.

The Interaction Formula

For the sake of generality and, at the same time, of simplicity in the derivation of the interaction formula, equations (1) and (5) may be written

$$(\tau_{cr})_{p=0} = K_2 L^n f_2(d,t) \tag{6}$$

$$-(p_{cr})_{\tau=0} = K_1 L^m f_1(d,t) \tag{7}$$

where K_1 and K_2 are arbitrary constants, m and n are arbitrary exponents, and f_1 and f_2 are arbitrary functions of diameter and thickness. Elimination of L gives

$$-(p_{cr})_{\tau=0} = K_1 f_1 \left[\frac{(\tau_{cr})_{p=0}}{K_2 f_2}\right]^{m/n}$$

This equation is the formula for the curve of figure 6, which is a plot of τ_{cr} against $p - (p_{cr})_{\tau=0}$ and therefore, when $p = 0$, a plot of $(\tau_{cr})_{p=0}$ against $-(p_{cr})_{\tau=0}$. In order to find the interaction formula, substitute $p - (p_{cr})_{\tau=0}$ in place of $-(p_{cr})_{\tau=0}$ and τ_{cr} in place of $(\tau_{cr})_{p=0}$ and simplify the resulting expression. Thus,

$$p - (p_{cr})_{\tau=0} = K_1 f_1 \left(\frac{\tau_{cr}}{K_2 f_2}\right)^{m/n}$$

Dividing through by $-(p_{cr})_{\tau=0}$ and using equations (6) and (7) yields

$$-\frac{p}{(p_{cr})_{\tau=0}} + 1 = \frac{K_1 f_1}{K_1 L^m f_1}\left(\frac{\tau_{cr}}{K_2 f_2}\right)^{m/n} = \left[\frac{\tau_{cr}}{(\tau_{cr})_{p=0}}\right]^{m/n}$$

A rearrangement of terms gives

$$\left[\frac{\tau_{cr}}{(\tau_{cr})_{p=0}}\right]^{m/n} + \frac{p}{(p_{cr})_{\tau=0}} = 1$$

If Donnell's equation (1a) is used with equation (5),

$$\frac{m}{n} = \frac{1}{0.53} = 1.89$$

or if Donnell's equation (1b) and equation (5) are used,

$$\frac{m}{n} = \frac{1}{0.5} = 2$$

Use of Lundquist's equation (3) with equation (5) yields

$$\frac{m}{n} = \frac{1}{0.46} = 2.17$$

For purposes of simplification, let

$$R_s = \frac{\tau_{cr}}{(\tau_{cr})_{p=0}}$$

$$R_p = \frac{p}{(p_{cr})_{\tau=0}}$$

and

$$q = \frac{m}{n}$$

Then, the final formula may be written

$$R_s^{\,q} + R_p = 1$$

APPENDIX B

APPLICATION OF INTERACTION FORMULA TO CURVED PANELS

The theoretical analysis of the buckling of a curved panel is much more difficult than the treatment of complete cylinders. In the case of buckling under torsion alone, the boundary conditions required for panels greatly complicate the theoretical analysis. It may be presumed, however, that the added restraints make the critical stress higher than that of a complete cylinder of the same length, thickness, and curvature. The relation between the pressure and the direct stresses produced in the sheet is also much more complicated than in the case of a complete cylinder. The axial stresses depend on the area of the end bulkhead and on the areas of cross section of sheet and spar elements. It is difficult to draw conclusions regarding the relation of pressure to circumferential stresses. It is therefore not to be expected that an interaction formula established for complete cylinders will necessarily apply to curved sheet also.

In order to determine whether the interaction formula derived in appendix A may be used to gain a rough idea of the strengthening effect of internal pressure in the case of curved panels, the formula is applied to the test points of the two specimens of reference 2. Figure 8 is a sketch of the two specimens tested. In figure 9 the experimental shear buckling stresses are plotted against the internal pressure.

Curves representing the interaction formula are also plotted in figure 9. In order to apply the formula, the experimentally determined values of $(\tau_{cr})_{p=0}$ were used; $(p_{cr})_{\tau=0}$ is assumed to be the same as for a complete cylinder of identical length, thickness, and curvature, and is found by applying equation (4) of appendix A. Fair agreement was obtained between the curves and the test points and the agreement might be considerably improved by a more precise method of determining $(p_{cr})_{\tau=0}$.

REFERENCES

1. Rafel, Norman: Effect of Normal Pressure on the Critical Compressive Stress of Curved Sheet. NACA RB, Nov. 1942.

2. Rafel, Norman: Effect of Normal Pressure on the Critical Shear Stress of Curved Sheet. NACA RB, Jan. 1943.

3. Donnell, L. H.: Stability of Thin-Walled Tubes under Torsion. NACA Rep. No. 479, 1933.

4. Timoshenko, S.: Theory of Elastic Stability. McGraw-Hill Book Co., Inc., 1936, p. 450.

5. Lundquist, Eugene E.: Generalized Analysis of Experimental Observations in Problems of Elastic Stability. NACA TN No. 658, 1938.

6. Lundquist, Eugene E.: Strength Tests on Thin-Walled Duralumin Cylinders in Torsion. NACA TN No. 427, 1932.

7. Windenburg, Dwight F., and Trilling, Charles: Collapse by Instability of Thin Cylindrical Shells under External Pressure. Trans. A.S.M.E., APM-56-20, vol. 56, no. 11, Nov. 1934, pp. 819-825.

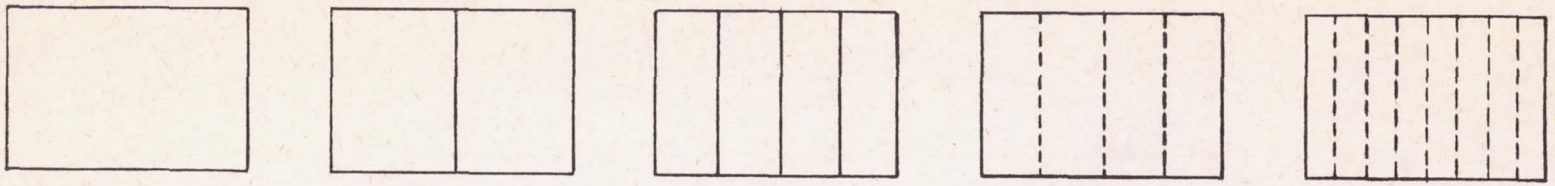

Cylinder 1
No rings

Cylinder 2
One ring at center

Cylinder 3a
Three rings equally spaced

Cylinder 3b
Three rings equally spaced

Cylinder 4
Seven rings equally spaced

Solid lines represent rings on inside and outside
Dotted lines represent rings on inside only

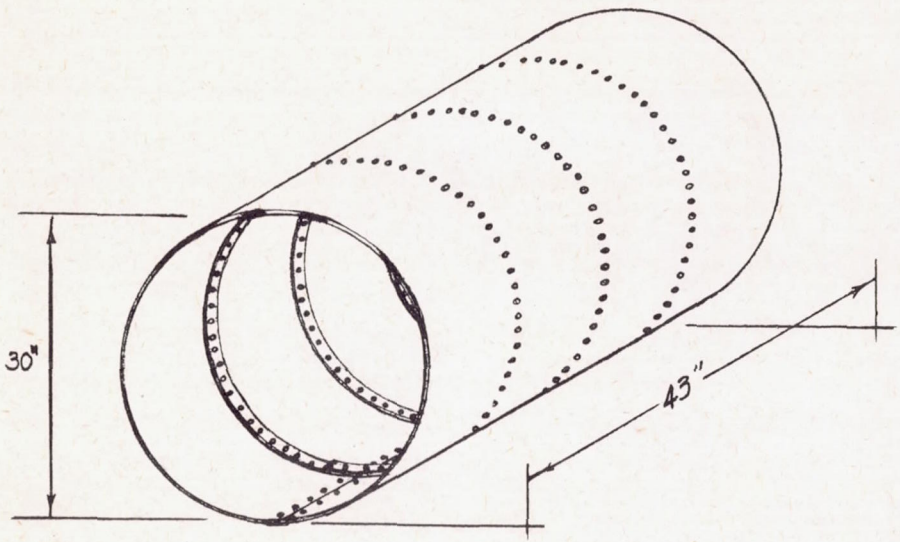

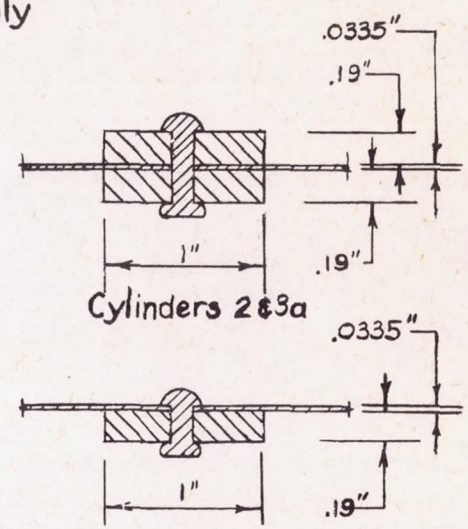

Cross sections at rings

Figure 1. - Test specimens.

NATIONAL ADVISORY
COMMITTEE FOR AERONAUTICS.

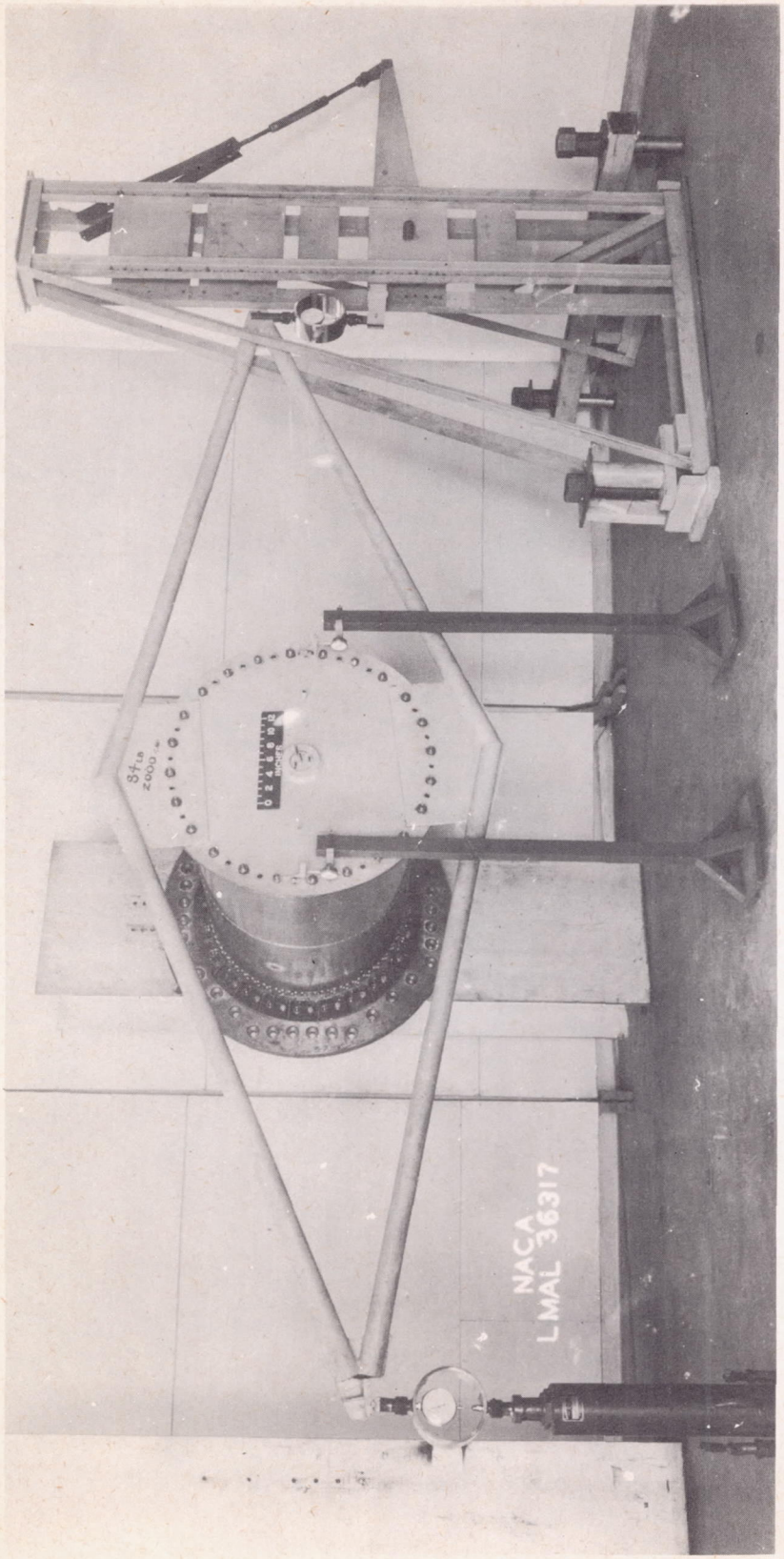

Figure 2.- Test setup.

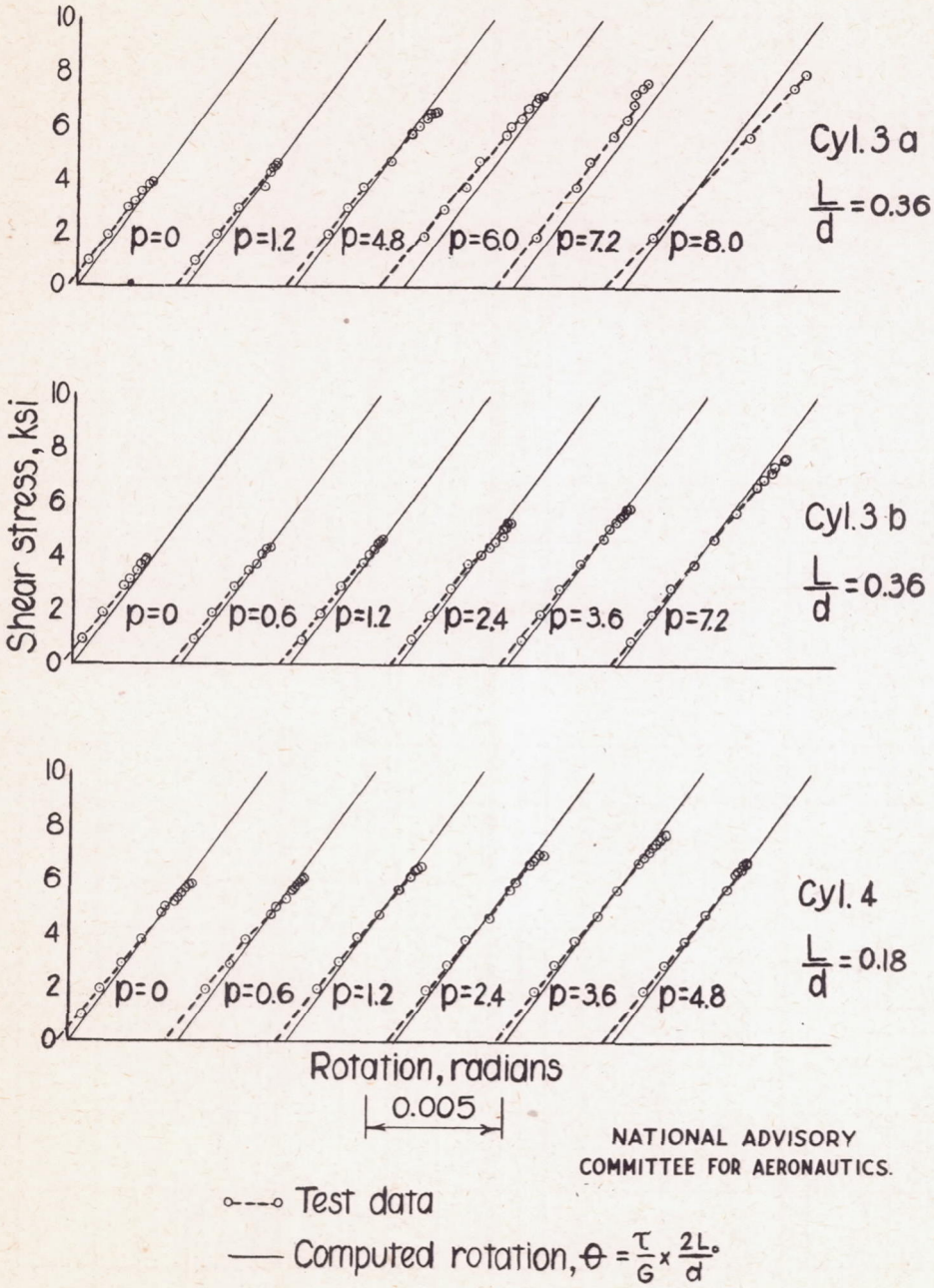

Figure 3.- Shear stress-rotation curves for cylinders with various ring spacings and internal pressures.

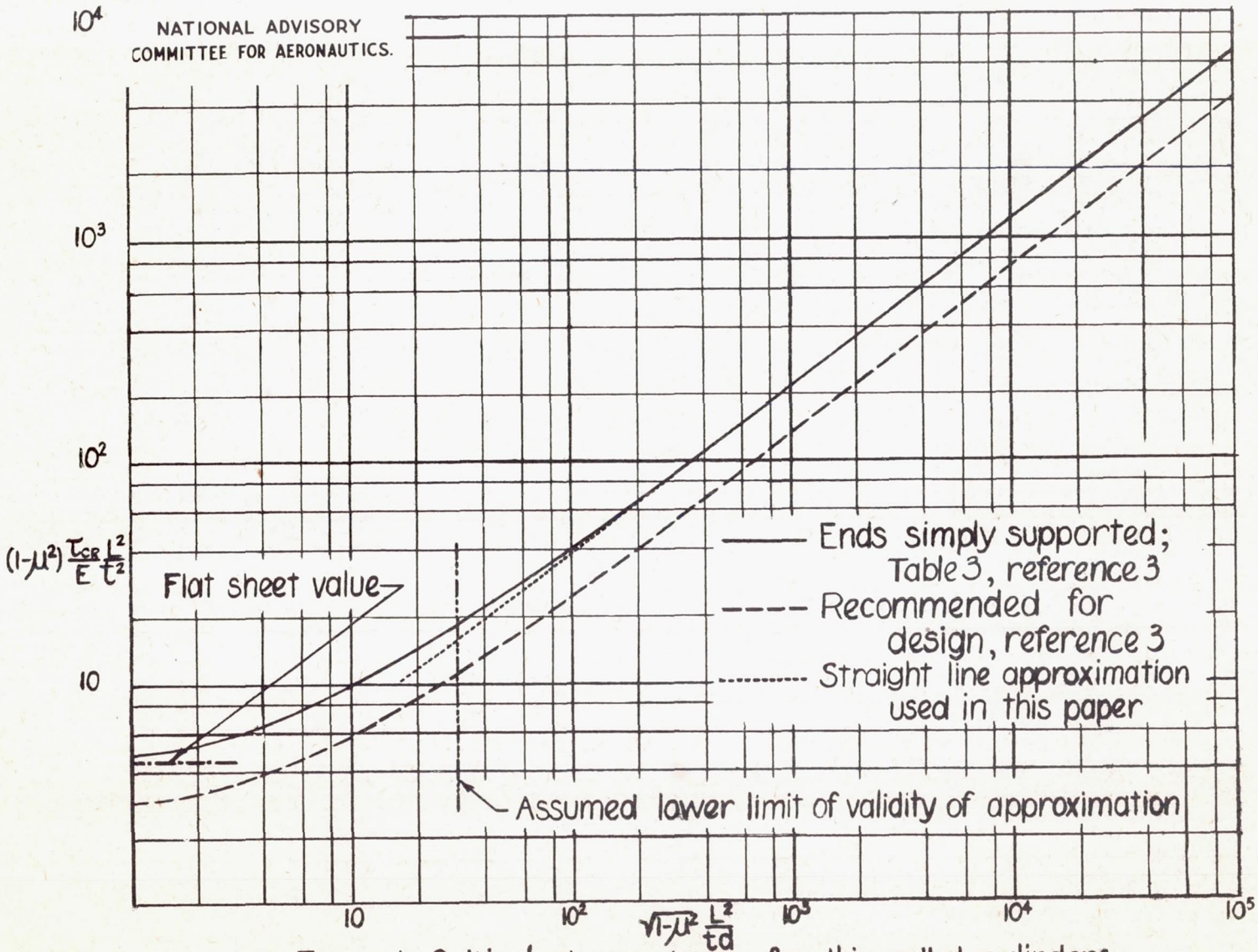

Figure 4.-Critical shear stress for thin-walled cylinders.

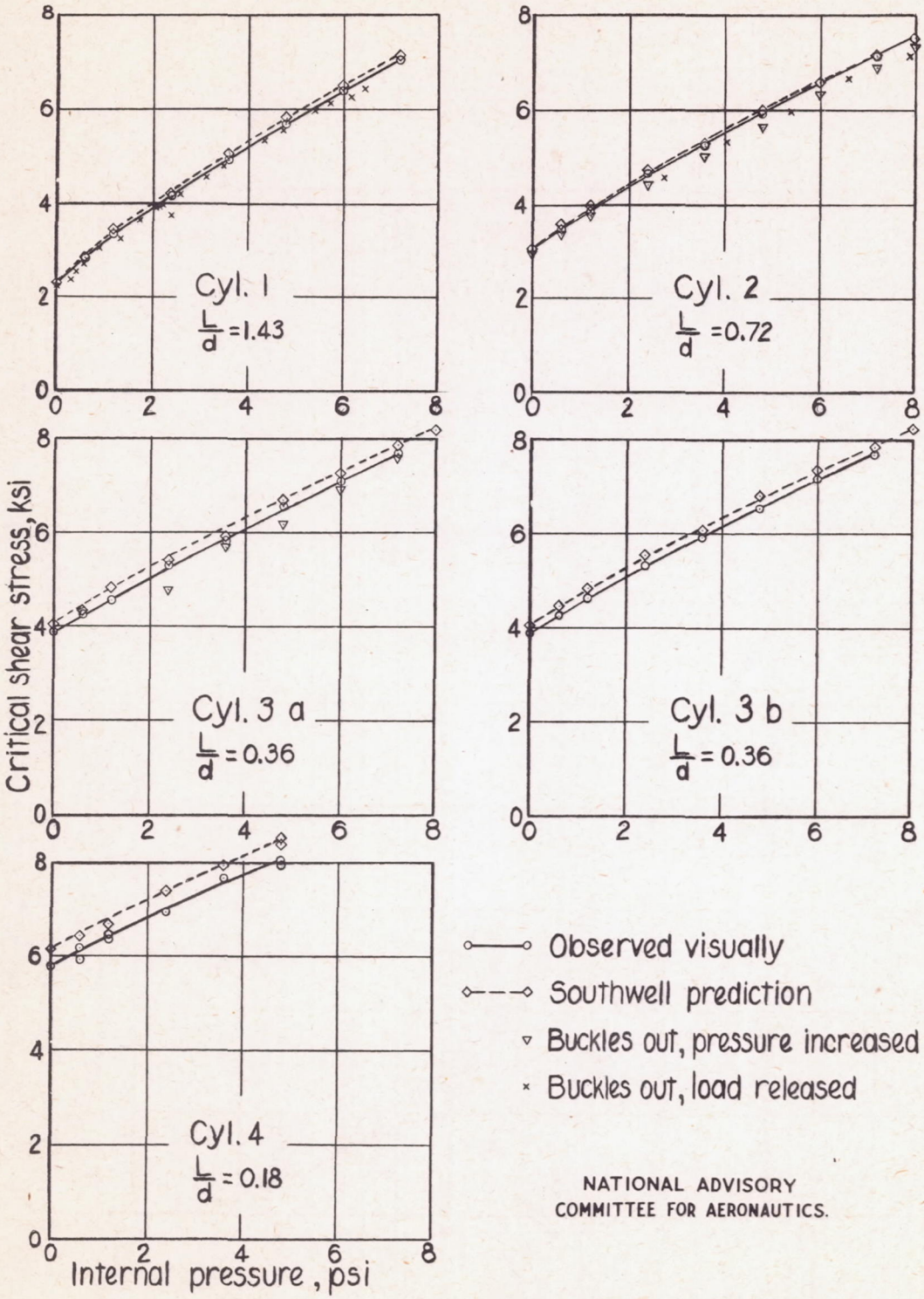

Figure 5.- Effect of internal pressure on critical shear stress for thin-walled circular cylinders.

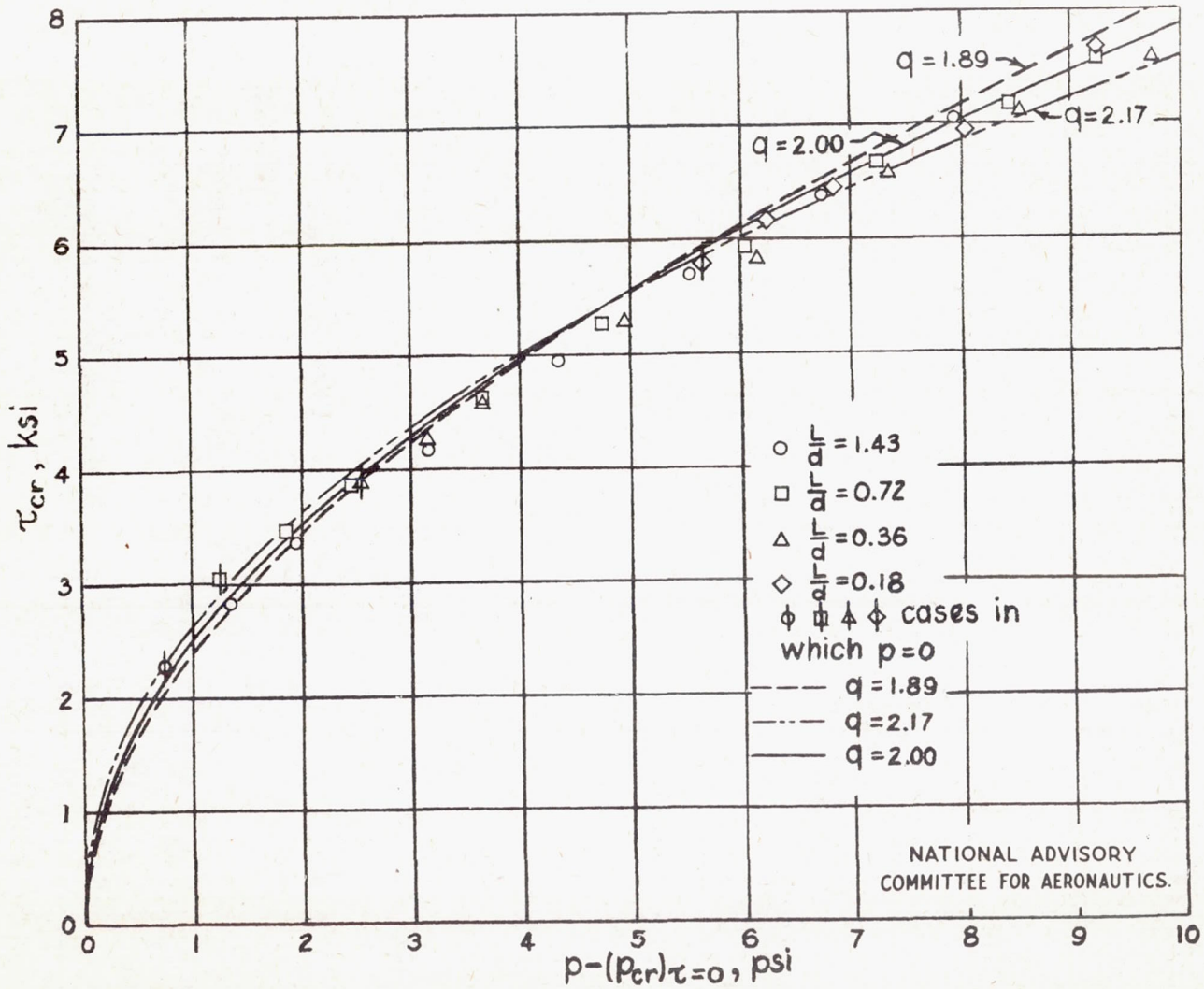

Figure 6.- Data of figure 5 plotted to adjusted scale and curves derived from interaction formula for various values of the exponent q.

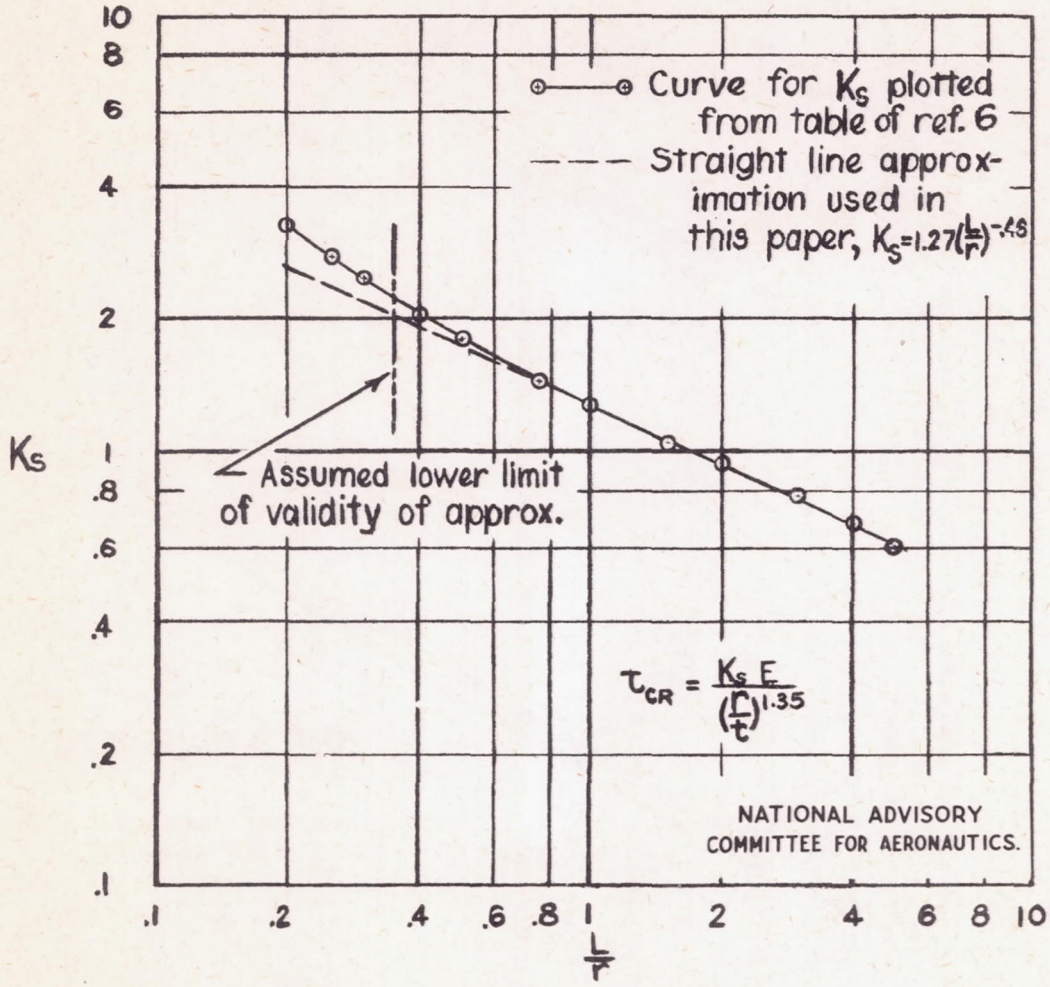

Figure 7.- Value of K_s used in empirical formula for critical shear stress of thin-walled cylinders.

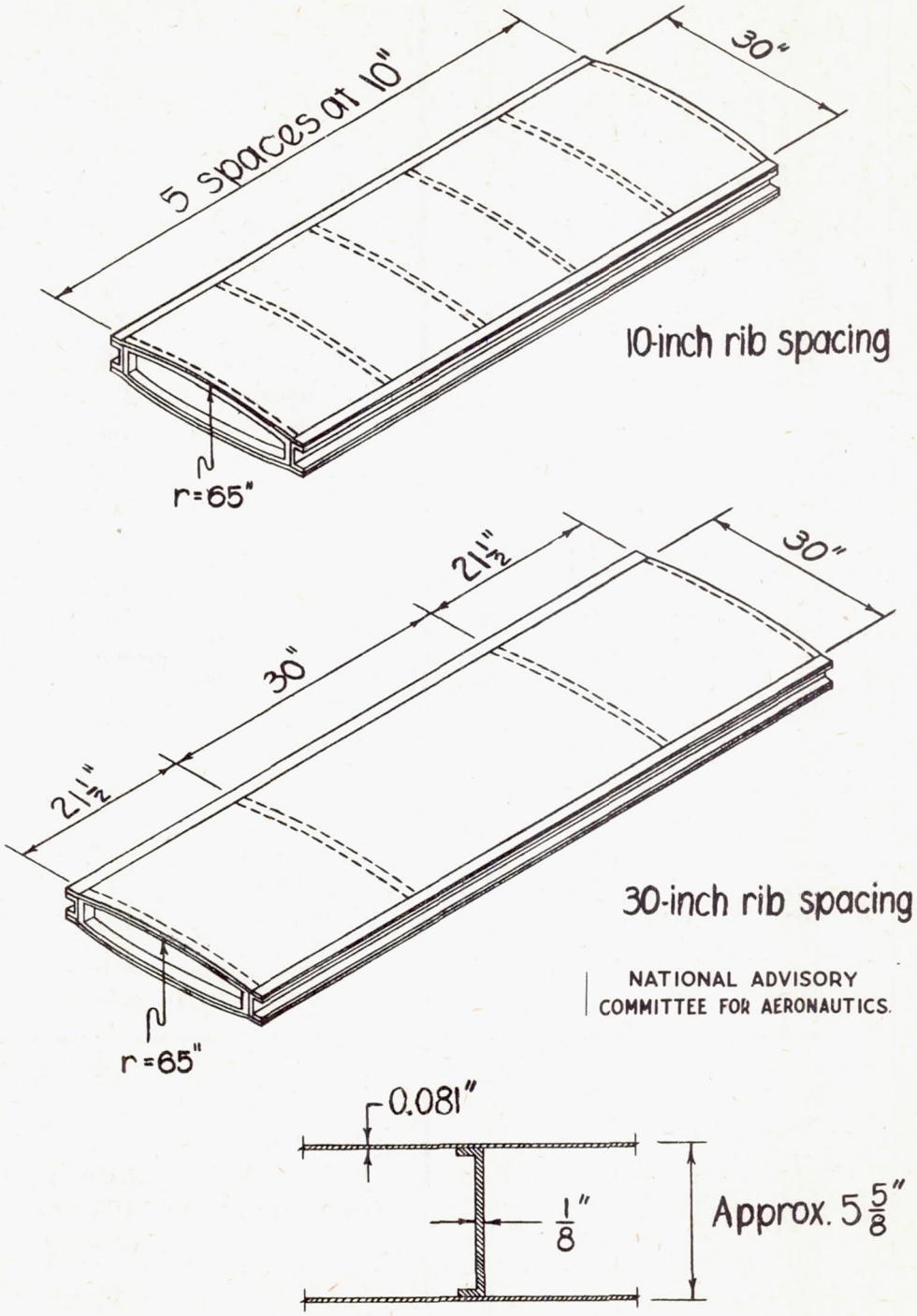

Figure 8.-Curved-sheet panels of reference 2.

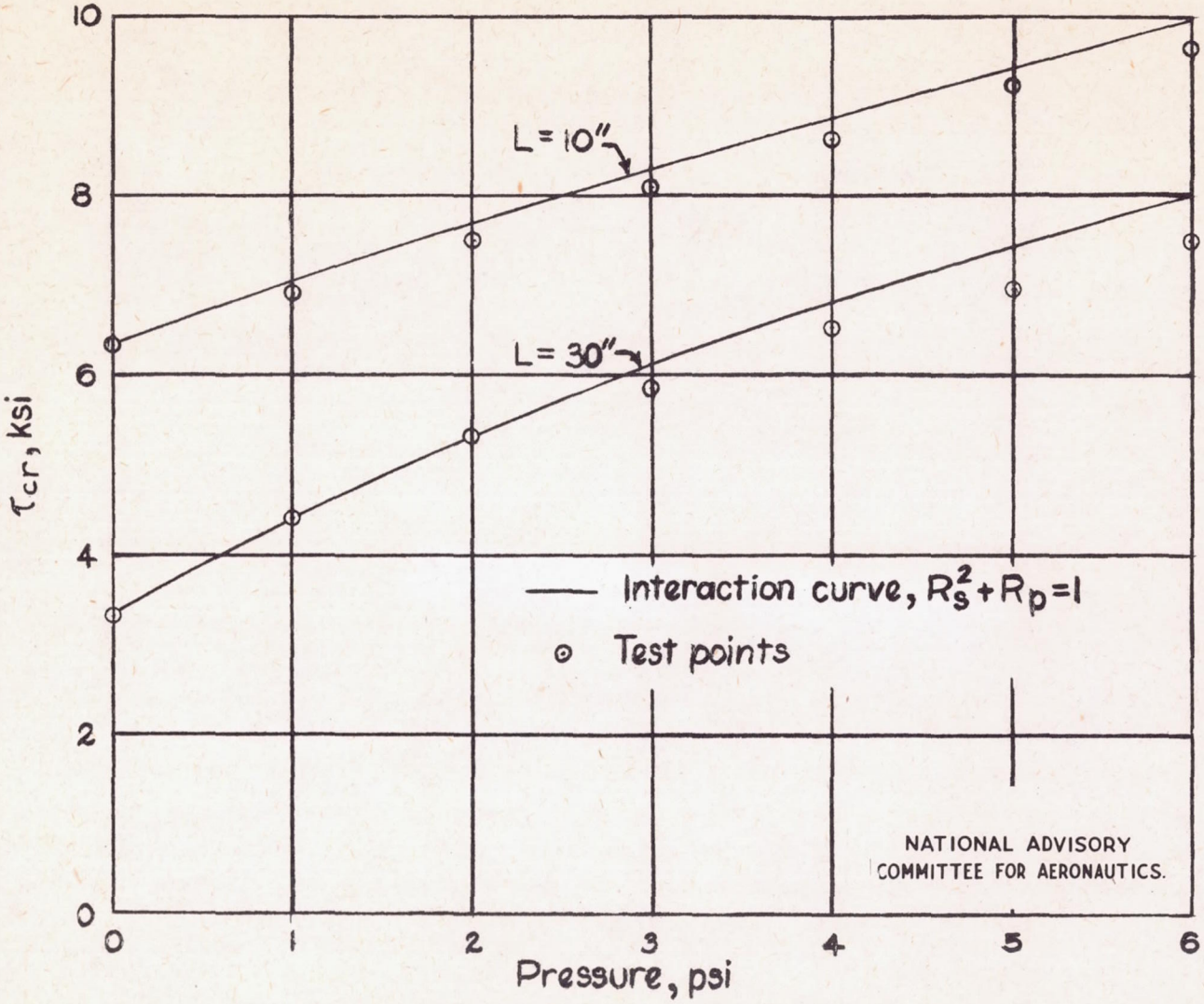

Figure 9.- Interaction formula applied to curved panel specimens of reference 2.